Journal Pre-proofs

Full length article

Quanta emission rate during speaking and coughing mediated by indoor temperature and humidity

Vitor Lavor, Jianjian Wei, Omduth Coceal, Sue Grimmond, Zhiwen Luo

PII: S0160-4120(25)00130-8
DOI: https://doi.org/10.1016/j.envint.2025.109379
Reference: EI 109379

To appear in: *Environment International*

Received Date: 29 October 2024
Revised Date: 4 March 2025
Accepted Date: 13 March 2025

Please cite this article as: V. Lavor, J. Wei, O. Coceal, S. Grimmond, Z. Luo, Quanta emission rate during speaking and coughing mediated by indoor temperature and humidity, *Environment International* (2025), doi: https://doi.org/10.1016/j.envint.2025.109379

Quanta emission rate during speaking and coughing mediated by indoor temperature and humidity

Vitor Lavor[1], Jianjian Wei[2], Omduth Coceal[3], Sue Grimmond[3], Zhiwen Luo[4,*]

[1] School of the Built Environment, University of Reading, Reading, UK

[2] Institute of Refrigeration and Cryogenics, Key Laboratory of Refrigeration and Cryogenics Technology of Zhejiang Province, Zhejiang University, Hangzhou, China

[3] Department of Meteorology, University of Reading, Reading, UK

[4] Welsh School of Architecture, Cardiff University, Cardiff, UK

[*] Correspondence: luoz18@cardiff.ac.uk

Abstract

In epidemiological prospective modelling, assessing the hypothetical infectious quanta emission rate (E_q) is critical for estimating airborne infection risk. Existing E_q models overlook environmental factors such as indoor relative humidity (RH) and temperature (T), despite their importance to droplet evaporation dynamics. Here we include these environmental factors in a prospective E_q model based on the airborne probability functions with emitted droplet distribution for speaking and coughing activities. Our results show relative humidity and temperature have substantial influence on E_q. Drier environments exhibit a notable increase in suspended droplets (cf. moist environments), with E_q having a 10-fold increase when RH decreases from 90 % to 20 % for coughing and a 2-fold increase for speaking at a representative summer temperature (T = 25° C). In warmer environments, E_q values are consistently higher (cf. colder), with increases of up to 22 % for coughing and 9 % for speaking. This indicates temperature has a smaller impact than humidity. We demonstrate that indoor environmental conditions are important when quantifying the quanta emission rate using a prospective method. This is essential for assessing airborne infection risk.

Keywords: Expiratory droplets; Quanta emission rate; Quanta; Indoor, Long-range airborne transmission

Highlights

- RH and temperature are important factors to estimate quanta emission rate (E_q)
- In dry environments, E_q for coughing increases ~10-fold and speaking 2-fold
- In dry summer conditions, higher temperature can increase E_q up to 22 %
- Medium-sized droplets may play a key role in infection transmission via inhalation

Graphical abstract

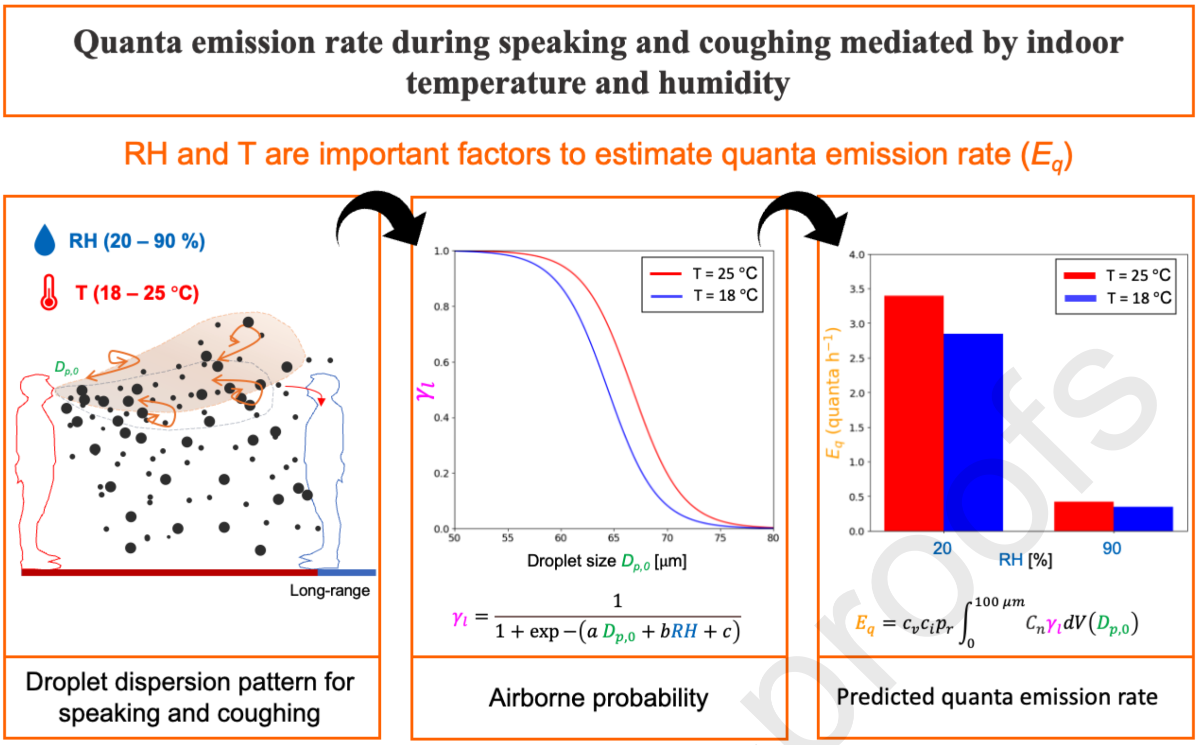

Nomenclature

Variable	Meaning	Reference	Unit
A_r	Attack rate	Eq. 10	%
a, b, c	Fitted parameters in the sigmoid function	Eq. 6	-
c_i	Conversion factor	Eq. 1	Quanta RNA copies^{-1}
C_n	Droplet number concentration	Eq. 2, 4	Particles m^{-3}
c_v	Viral load	Eq. 1	RNA copies mL^{-1}
D_{crit}	Maximum diameter of exhaled droplet	Eq. 2	μm
$D_{i,med}$	Count median diameter	Eq. 4	μm
$D_{i,sd}$	Geometric standard deviation	Eq. 4	μm
$D_{p,0}$	Initial diameter of droplets	Eq. 2	μm

E_q	Quanta emission rate	Eq. 1, 10	Quanta h^{-1}
I	Number of infectors	Eq. 10	person
n	Number of samples	Eq. 7-9	-
N_{total}	Number of droplets released	Eq. 5	-
N_{ground}	Number of droplets that settle to the ground	Eq. 5	-
p_r	Pulmonary ventilation rate	Eq. 1, 10	$m^3 h^{-1}$
t_{ex}	Exposure time	Eq. 10	h
T	Temperature	Eq. 3	ºC
v	Volume concentration	Eq. 1	mL m^{-3}
V	Volume of a single droplet	Eq. 2	mL
V_{venue}	Volume of the venue	Eq. 10	m^3
x	Horizontal distance	Eq. 5	m
y_i	“True” value	Eq. 7-9	-
$\hat{y}_i$	Predicted value	Eq. 7-9	-
$\bar{y}_i$	Mean “true” value	Eq. 7-9	-
λ	Air changes per hour	Eq. 10	h^{-1}
γ	Airborne probability	Eq. 5	-
γ_l	Long-range airborne probability	Eq. 3, 6	-
MAE	Mean absolute error	Eq. 7	-

MBE	Mean biased error	Eq. 8	-
RH	Relative humidity	Eq. 3	%
R^2	Coefficient of determination	Eq. 9	-

1. Introduction

Transmission routes of respiratory pathogens are determined by how infectious respiratory particles (IRP) travel through the environment and how exposed people interact with them (Marr & Tang, 2021). The World Health Organization (WHO) suggests the terminologies of airborne (or inhalation), direct deposition and contact for the major modes of transmission of respiratory pathogens (Leung & Milton, 2024). The inhalation/airborne route occurs when expelled IRPs are inhaled and deposited in any site of the human respiratory tract, with can be subdivided into: (1) short-range: involving inhaling IRPs in close proximity (<1-2 m) (Y. Li, 2021a), and (2) long-range: referring to inhalation of aerosols at greater distances (Duval et al., 2022).

Infection transmission risk can be estimated using Quantitative Microbial Risk Assessment (QMRA), with a dose-response model to predict the likelihood of infection based on exposure to a certain dose of pathogens (Sze To & Chao, 2010). The Wells-Riley equation, one of the most used QRMA methods for evaluating airborne infections, quantifies the risk probability by considering variables such as ventilation rate, exposure time and quanta emission rate (E_q) (Kurnitski et al., 2021). The Wells (1955) dimensionless quantum of contagion represents the infectious dose necessary to infect 63.2 % of susceptible individuals [i.e., (1 – 1/e)] with pathogens-to-quanta ratio varying by pathogen type (Mikszewski et al., 2022). The quantum accounts for both concentration and virulence of the infectious material in the air. The rate infectious quanta are released into the air from a person (E_q) is essential for modelling the spread of airborne diseases and implementing effective control methods (Jones et al., 2023).

Generally, two methods are used for estimating E_q. First, the retrospective method uses a past contamination airborne transmission outbreak event to estimate E_q from epidemiological factors and ventilation rates (Miller et al., 2021). The outbreak data needed includes ventilation conditions (mechanical/natural ventilation), population density and behaviours, and ambient conditions. Insights derived from post-event data alone may be potentially delayed and could result in inaccurate estimates. Scarce data about variability of emission rates between emitters and through time may limit ability to extrapolate to other scenarios (Jones et al., 2024). Second, the prospective method (Buonanno, Stabile, and Morawska, 2020) estimates E_q using the viral load from IRPs and pathogen's infectivity data from measurements (e.g., aerosol samples and RT-qPCR (Stadnytskyi et al., 2020)), making it more reliable and applicable to various studies (Buonanno et al., 2022; J. Li et al., 2021; Mikszewski et al., 2022).

The prospective method quanta emission rate (E_q) [quanta h^{-1}] is estimated from (Buonanno, Stabile, and Morawska, 2020):

$$E_q = c_v c_i p_r v \tag{1}$$

where c_v is the viral load of exhaled droplets [deoxyribonucleic acid (RNA) copies mL^{-1}], c_i is the conversion factor [quanta RNA $copies^{-1}$], and p_r is the pulmonary ventilation rate of the infected person [$m^3 h^{-1}$]. The volume concentration of exhaled droplets [mL m^{-3}], v, is calculated by integrating over the volumes of droplets of initial diameter $D_{p,0}$:

$$v = \int_0^{D_{crit}} C_n(D_{p,0}) dV(D_{p,0}) \quad (2)$$

where C_n is the droplet number concentration [particles m^{-3}] and V is the volume of a single droplet [mL]. The critical droplet diameter [µm], D_{crit}, is essential for understanding particle behaviour dynamics in respiratory emissions. For a given ambient condition, D_{crit} indicates the threshold between droplets with $D_{p,0} > D_{crit}$ that settles due to gravity and droplets with $D_{p,0} > D_{crit}$ that evaporate fully before settling (Chaudhuri et al., 2020; Xie et al., 2007). D_{crit} indicates the boundary between the inhalation/airborne to other transmission modes, since the former involves droplets that no longer remain suspended in the air.

Buonanno et al. (2020) originally used a D_{crit} of 10 µm, while Li et al. (2021) used 20 µm suggesting only IRPs that shrink to around 5-10 µm in diameter should be accounted for in the inhalation transmission route. These D_{crit} values were likely chosen for simplicity, assuming that inhalation transmission occurs only if IRPs are < 5 µm in diameter (Y. Li et al., 2022). This is now considered outdated (Jimenez et al., 2022), as there is evidence that IRPs dynamics are environment-dependent, with settling rate and spread distance influenced by various factors including droplet size, internal content, exhalation mode, speed and direction, expired jet flow instabilities, ambient air temperature (T) and relative humidity (RH) (Cavazzuti & Tartarini, 2023; Chaudhuri et al., 2020; Liu et al., 2017; Wei & Li, 2015). For example, Xie et al. (2007) demonstrate D_{crit} could vary from 95 to 65 µm (for RH of 30 % and 70 %) in an indoor environment with T = 20 ºC, while Chaudhuri et al. (2020) found D_{crit} can almost double when the indoor environment warmed from 5 to 35 ºC. Turbulence-induced exhaled jet fluctuations in droplet dispersion can cause up to a four-fold greater spread compared to cases where turbulence is disregarded (Wei & Li, 2015). Despite evidence of their importance, environmental characteristics are overlooked in estimating E_q from both retrospective and prospective methods.

To better understand how indoor environmental factors influence the critical droplet diameter and hence E_q, we use a prospective approach and integrate the airborne probability of respirable-sized IRPs after modelling evaporation and transport for different indoor RH and T scenarios. The model results are used for deriving a simple parametrization for airborne probability in relation to environment conditions, to calculate E_q. We utilise our modified E_q to simulate different outbreaks, which we compare to the classic Buonanno et al. (2020) case.

2. Methods

2.1 Modified quanta emission rate *(E_q)* estimation

Our modified prospective method is developed to improve understanding of how indoor environmental conditions affects E_q.

$$E_q = c_v c_i p_r \int_0^{D_{crit} = 100\ \mu m} C_n(D_{p,0}) \gamma_l(D_{p,0}, RH, T) dV(D_{p,0}) \quad (3)$$

where γ_l is the airborne probability of droplets (Section 2.1.2). We consider both relative humidity (RH) in the range 20 to 100 % and indoor air temperature (T) of 18 and 25 ºC to represent summer and winter indoor conditions of temperature-controlled environments in Europe (Salthammer & Morrison, 2022).

If IRPs settle on the ground, they no longer represent an inhalation transmission route risk. Hence, we include airborne probability (Wei & Li, 2015) to indicate the likelihood of

IRPs remaining suspended in the air rather than settling at a specific distance (Grandoni et al., 2024; Wei & Li, 2015).

We set the upper limit of droplet size that can be inhaled by humans to 100 µm (Milton, 2020) as a more realistic cut-off for D_{crit} for the inhalation route. Turbulence can enhance the dispersion and spread of expired IRPs and this is captured by the airborne probability, as large dried-out droplets (> 50 µm) can be found up to 4 m from the emitter when coughing is considered (Wei & Li, 2015). Even low probabilities of larger droplets reaching longer distances may have important implications for the airborne disease transmission.

2.1.1 Droplet size distribution

We adopt Johnson et al. (2011)'s droplet number concentration (C_n) from their trimodal distribution (Table 1) for speaking and coughing activities. It allows IRPs to be released from different origins in the respiratory tract, including bronchiolar, laryngeal, and oral sites.

$$\frac{dC_n}{dLog\ D_{p,0}} = \ln(10)\ x \sum_{i=1}^{3}\left(\frac{C_{n,i}}{\sqrt{2\pi}\ln(D_{i,sd})}\right)\exp\left(-\frac{\left(\ln D_{p,0} - \ln(D_{i,med})\right)^2}{2\left(\ln D_{i,sd}\right)^2}\right) \tag{4}$$

Table 1. Trimodal droplet size distribution model parameters for coughing and speaking (Johnson et al., 2011) including diameter geometric standard deviation ($D_{i,sd}$) and count median diameter ($D_{i,med}$).

	Coughing			Speaking		
Mode	Bronchiolar	Laryngeal	Oral	Bronchiolar	Laryngeal	Oral
C_n [cm^{-3}]	0.0903	0.1419	0.0159	0.054	0.0684	0.00126
$D_{i,med}$ [µm]	2.4123	2.4615	123.3	2.4830	3.6923	144.6
$D_{i,sd}$ [µm]	1.25	1.68	1.837	1.30	1.66	1.795

2.1.2 Airborne probability (γ)

Droplets that settle on the ground are removed from the air, so no longer represent an inhalation transmission risk. By introducing the airborne probability of droplets (γ) we consider turbulence-induced exhaled jet fluctuations and their impact on dispersion using a discrete random walk approach. The γ term gives the likelihood of IRPs remaining suspended in the air, by the quantity that settle to the ground, $N_{ground}(x)$, at a specific distance *x* relative to the total number of droplets released, N_{total} (Grandoni et al., 2024; Wei & Li, 2015):

$$\gamma = 1 - \frac{N_{ground}(x)}{N_{total}} \tag{5}$$

As we consider only IRPs inhaled at a long-range, we calculate the long-range airborne probability (γ_l) for speaking using x = 2 m. For coughing a larger threshold of x = 4 m is adopted, as the cough jet can remain suspended in the air for longer compared to speaking breaths (Bourouiba, 2020).

2.1.3 Droplet movement and evaporation

The long-range airborne probability (γ_l) requires information of movement and evaporation of exhaled IRPs to be modelled. The initial velocity of an exhaled droplet depends on respiratory activity. Once exhaled evaporation will cause the droplet to start to lose water to the ambient air. Key model assumptions are (details in Appendix and Wei & Li, 2015):

- Exhaled droplets are spherical during transport.
- Thermophysical properties are uniform within the droplet.
- Heat transfer processes through the droplet surface are convective heating and evaporative cooling.
- Exhaled droplets contain both soluble and insoluble components. Vapour pressure at the droplet surface depend on Kelvin and solute effects.
- Droplets are emitted together with breathing air in a turbulent buoyant round jet, with a discrete random walk representing in-jet turbulence.

2.2 Cases simulated

The two indoor air temperatures considered, warm (T = 25 ºC) and cool (T =18 ºC), are intended to represent typical summer and winter indoor conditions in temperature-controlled environments in Europe (Salthammer & Morrison, 2022). Obviously, values vary associated with regional and cultural factors. Eight relative humidity conditions are selected to cover a range of indoor humidity scenarios. These span 20 to 90 %, at 10% intervals. The exhaled droplets range in diameter from 10 to 100 μm (interval = 2 μm), aligning with the upper limit of droplet diameter that can be inhaled by humans (Milton, 2020).

The epidemiological parameters are fixed for all simulations to estimate the quanta emission rate, using the volume concentration from Eq. 2. The median epidemiological parameter values for SARS-CoV-2 are used for viral load c_v (= 4×10^5 RNA copies mL^{-1}) and conversion factor c_i (= 0.0014 quanta RNA^{-1}) (Mikszewski et al., 2022). Pulmonary ventilation rate p_r varies with respiratory activities, with speaking being 0.54 m^3 h^{-1} (Mikszewski et al., 2022) and for coughing being 0.0144 m^3 h^{-1} based on persistent coughing [frequency 9 coughs h^{-1}] with a coughing flow rates of 2.45×10^{-3} m^3 cough^{-1} (Altshuler et al., 2023; Gupta et al., 2009). We use a constant coughing frequency of 9 per hour, whereas this can vary with contamination stage and pathogen (Altshuler et al., 2023).

Quanta emission rate is estimated based on the long-range airborne probability (Eq. 5) with 1000 exhaled droplets per simulation scenario. The exhalation velocity is kept constant at 5 (speaking) and 10 m s^{-1} (coughing) with an exhaled air temperature set at 35 ºC.

2.2.1 Parameterisation of long-range airborne probability (γ_l)

For computational efficiency a sigmoid equation is fit to the long-range airborne probability cases simulated:

$$\gamma_l = \frac{1}{1 + \exp\, -(a\, D_{p,0} + bRH + c)} \tag{6}$$

where a, b and c are the fitted parameters. The sigmoid function provides a smooth, continuous approximation of the probability, capturing nonlinear relationship between the settling and evaporation processes. This allows a fast airborne probability estimate across the range of droplet sizes without needing detailed calculations, thus reducing computational resources needed.

With only two indoor temperature scenarios, parameters are derived for each reparatory activity and temperature condition (i.e., four set of parameters or equations). The parameter fitting is done twice, with the results split by RH value into one (i.e. 20 - 90%), and three (low: 20 – 40 %, medium: 50 – 60 % and high: 70 – 90 %) classes.

The fitted model accuracy is evaluated by assessing the predictive capacity for RH values used in the training (fitting) phase, using standard metrics:

(1) Mean absolute error (MAE):

$$\mathrm{MAE} = \frac{1}{n}\sum_{i=1}^{n}|y_i - \hat{y}_i| \tag{7}$$

(2) Mean biased error (MBE):

$$\mathrm{MBE} = \frac{1}{n}\sum_{i=1}^{n}(y_i - \hat{y}_i) \tag{8}$$

(3) Coefficient of determination (R^2):

$$\mathrm{R}^2 = \frac{\sum_{i=1}^{n}(y_i - \hat{y}_i)^2}{\sum_{i=1}^{n}(y_i - \bar{y})} \qquad \bar{y}_i = \frac{1}{n}\sum_{i=1}^{n} y_i \tag{9}$$

where $\hat{y}_i$ is the predicted value of the i-th sample, with y_i is the "true" value, and $\bar{y}$ is the mean of the true values.

2.3 Application to two outbreak case studies

We compare our results to retrospective assessments from two SARs-CoV-2 outbreak cases: an outbreak in a restaurant in Guangzhou, China (Lu et al., 2020) and in a call centre in South Korea (Prentiss et al., 2020). In the retrospective analysis, we estimate the quanta emission rate using the Wells-Riley equation, considering no other losses apart from ventilation at the time of the event:

$$A_r = 1 - \exp\left(\frac{I p_r E_q t_{ex}}{V_{venue}\lambda}\right) \tag{10}$$

where A_r is the attack rate [%], I is the number of infectors [person], p_r is the pulmonary ventilation rate [$m^3\ h^{-1}$], E_q is the quanta generation rate [quanta (h person)$^{-1}$], t_{ex} is the exposure time interval [h], V_{venue} is the volume of the venue [m^3] and λ is the air changes per hour [h^{-1}].

Monte Carlo simulations (Kroese et al., 2014) are performed to estimate the E_q for retrospective method for each outbreak location. Parameters from Eq. 10 are used in the range values and distribution specified in Table 2, where uncertainties are obtained by varying there parameters within their specified lower and upper limits (Lu et al., 2020; Prentiss et al., 2020).

Table 2. Parametric values used in the Monte Carlo simulation for estimating E_q using the retrospective method in Equation 10 for a restaurant and a call centre (Lu et al., 2020; Prentiss et al., 2020).

Parameter	Restaurant China		Call Centre Korea	
	Values	***Distribution***	***Values***	***Distribution***
A_r (%)	0.45 - 0.81	Uniform	0.50 – 0.75	Uniform
p_r (m^3 h^{-1})	0.49 - 1.38	Uniform	0.49 – 1.38	Uniform
λ (h^{-1})	0.56 – 0.77	Uniform	0.5 – 1.5	Uniform
V_{venue} (m^3)	45	Constant	1143	Constant
t_{ex} (h)	1	Constant	8	Constant

Additionally, Monte Carlo simulations are also conducted for our proposed method using parameters from Eq. 1. The range of variables and their distributions, as shown in Table 3, are used to capture the uncertainties. This approach facilitates the analysis of the uncertainty estimates derived from both methods.

Table 3. Parametric values used in the Monte Carlo simulation for estimating our proposed method in Eq. 1 for simulated scenarios.

Parameter	Summer		Winter	
	Values	***Distribution***	***Values***	***Distribution***
c_i (quanta RNA copies^{-1})	0.0014	Constant	0.0014	Constant
c_v (RNA copies mL^{-1})	5.6 (1.2)	Log_{10} normal (mean/std dev)	5.6 (1.2)	Log_{10} normal (mean/std dev)
p_r (m3 h-1)	0.49 - 1.38	Uniform	0.5 – 1.5	Uniform
v (mL m^{-3})	0.047	Constant	0.021	Constant

RH (%)	20	Constant	90	Constant

3. Results and Discussion

3.1 Droplet dispersion pattern

To determine the number of droplets needed to provide robust statistical results an initial sensitivity analysis (Fig. S.1) found a1,000 droplets to be enough. This involves releasing a single droplet every 0.04 s over a 40 s duration.

A snapshot of the droplet distribution in space at t = 40 s, with an initial size $D_{p,0}$ of 50 µm varies with humidity conditions (RH = 20 and 90 %) and between activity, speaking (Fig. 1a) and coughing activity (Fig. 1b), in the summer scenario (T = 25 ºC). Medium-sized droplets predominantly follow the cough jet under dry environments for both coughing and speaking, as higher evaporation rate in lower RH conditions prolongs the presence of larger exhaled droplets in the environment. Wei & Li (2015) also highlighted the significant effect of evaporation on medium-sized droplets for coughing, while variations in RH have minimal impact on the airborne probability of small (< 30 µm) and large droplets (> 60 µm). Smaller droplets tend to follow the jet airflow closely, while larger droplets settle more quickly to the ground.

For both speaking and coughing, when the RH = 20 %, the airborne probability remains at 100 % across all considered distances (Fig. 1), indicating a tendency for dried-out droplets to follow jet streamlines in dry environments. In contrast, for wet environments with RH = 90 %, droplets are observed to settle at around 0.25 m from the emitter during speaking and 0.50 m during coughing with airborne probability decreasing to 0.15 and 0.25 for the largest distances considered, respectively, indicating reduced spread in more humid conditions.

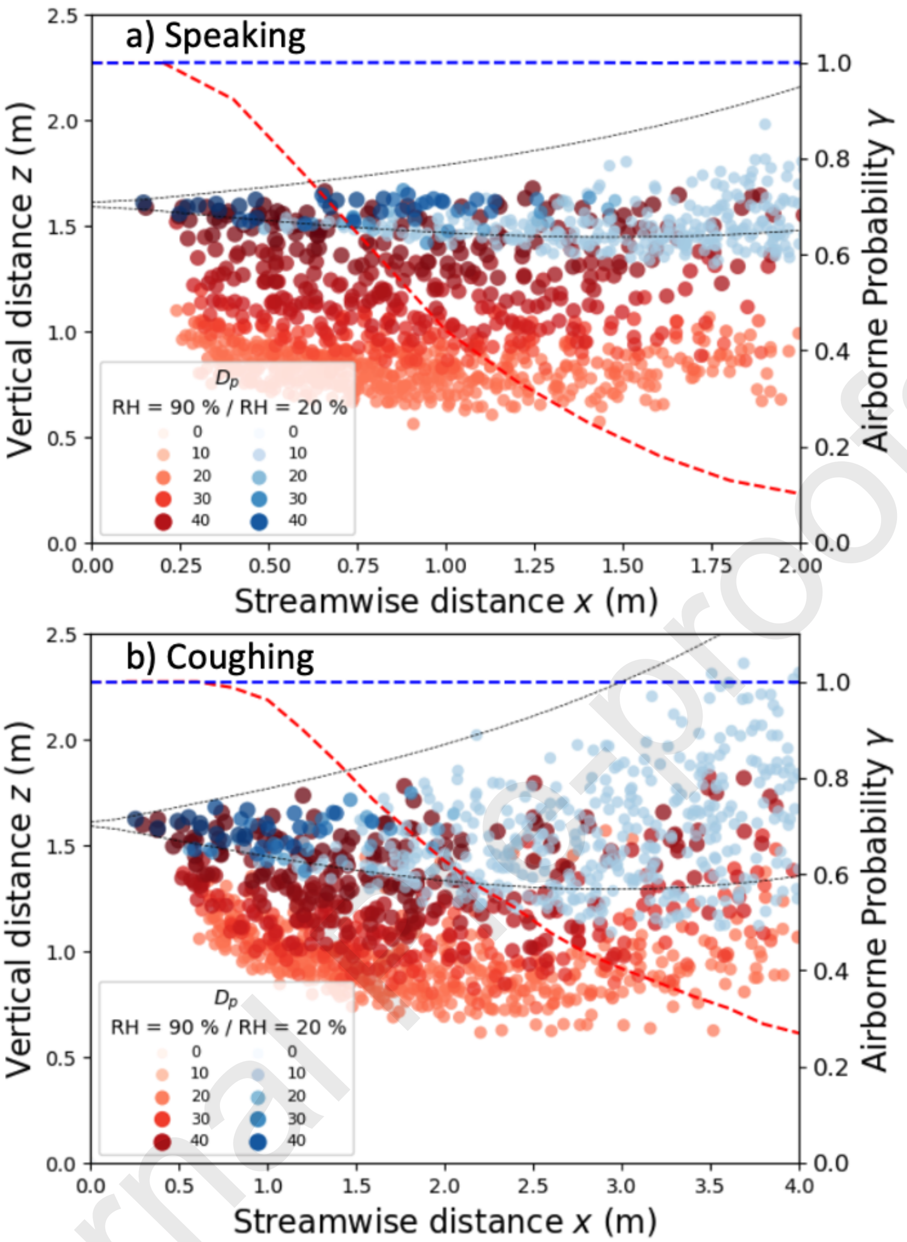

Figure 1. Droplet distribution at t = 40 s for (**a**) speaking and (**b**) coughing for two ambient RH conditions (blue: 20 %, red: 90 %) with expiratory jet boundaries (black dashed lines) and airborne probability (blue, red, dashed lines, right-hand y-axis). The initial droplet diameter is 50 µm and T = 25 ºC.

3.2 Long-range airborne probability of droplets

Long-range airborne probability of exhaled droplets (γ_l) is computed across various RH levels and droplet sizes for the winter and summer air temperatures. Threshold distances (x_t) are set to 2 m for speaking and 4 m for coughing, to allow the long-range inhalation route to be distinguished from the short-range (Eq. 5).

There is a consistent decline in γ_l with increasing droplet size and RH for both coughing and speaking activities (Fig. 2). Between γ_l = 0.02 (pink, Fig. 2) and green γ_l = 0.98 (green) is where most droplets are susceptible to fluctuation in long-range airborne probability. This indicates long-range airborne probability for medium-sized droplets (40 – 70 µm) are more influenced by external conditions, particularly in environments with low to medium RH (< 70 %). Although higher RH environments are expected to have fewer suspended droplets, a fraction of 50 μm droplets will persist (12.3 % for coughing and 6.6 %

for speaking, with the winter T). Larger droplets are more susceptible to indoor temperature variations, as evidenced by the leftward shift of the γ_l = 0.02 bound from summer (pink solid, Fig. 2) to winter (dashed) for both respiratory activities This shift indicates that droplets with same size evaporate more rapidly in higher temperature environments due to heightened vapour pressure deficit, resulting in a greater droplet suspension in the air.

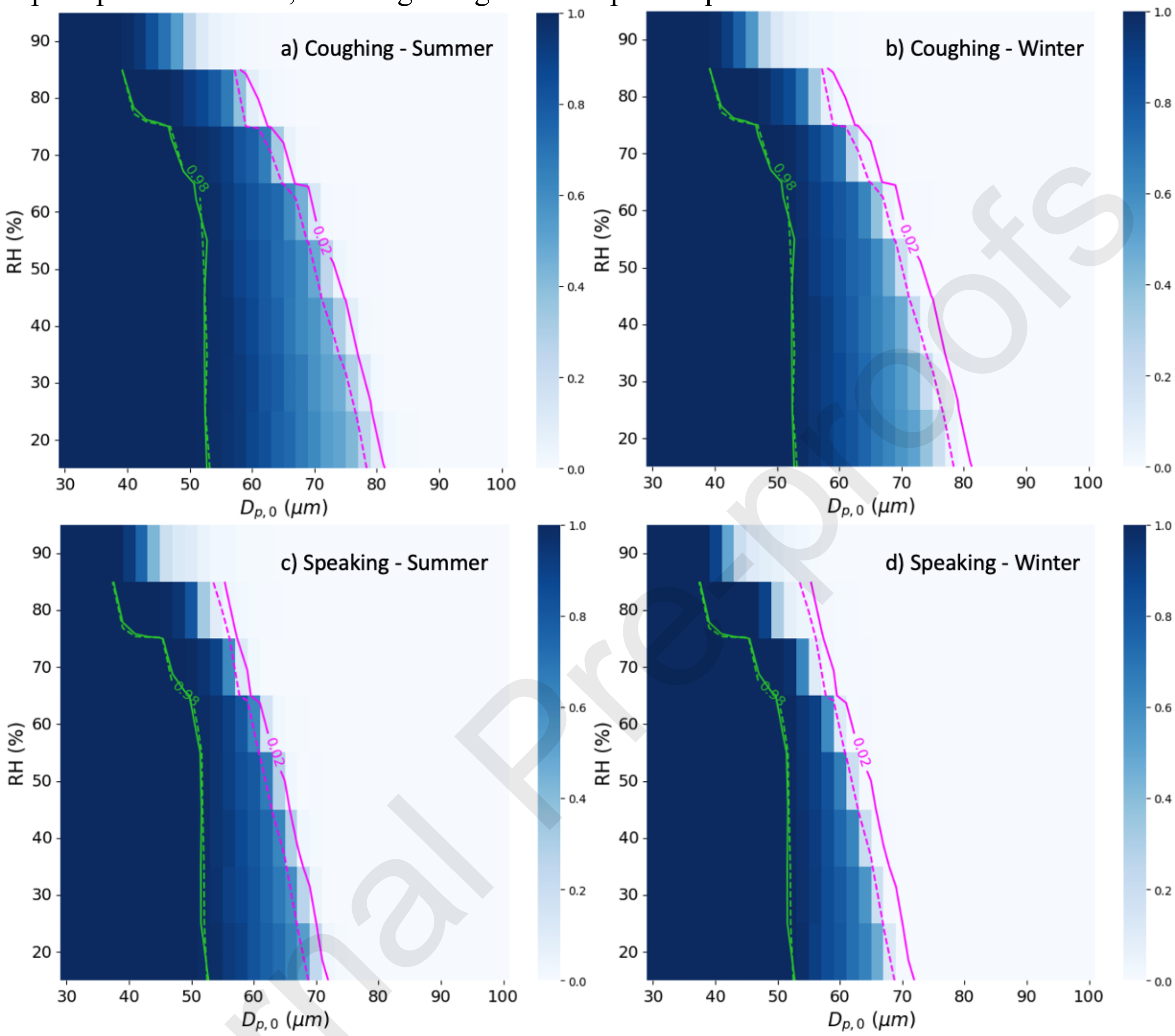

Figure 2. Heat map of γ_l in summer and winter for (a, b) coughing and (c, d) speaking with values γ_l of 0.02 (pink) and 0.98 (green) when is T = 25 °C (solid) and T = 18 °C (dashed).

The long-range airborne probability model parameters (Table 4) are derived from fitting Eq. 6 using One and Three RH classes approaches. The fits are verified using ambient RH of 35 % and 55 % (i.e. a low and medium case from the Three RH class approach), for data not used in the fitting stage.

Table 4. Fitted parameters for the sigmoid equation (Eq. 6) using the One and Three RH classes approaches for summer and winter temperatures.

Model	**Summer (T = 25 °C)**			**Winter (T = 18 °C)**		
	a	**b**	**c**	**a**	**b**	**c**

Coughing One	-0.2659	-0.0869	21.9210	-0.3028	-0.0974	24.3288
Speaking One	-0.4307	-0.1313	32.6496	-0.4976	-0.1470	36.5284
Coughing Three						
• Low RH	-0.2207	-0.0279	16.5011	-0.2525	-0.0319	18.4122
• Medium RH	-0.3262	-0.0707	25.8772	-0.3958	-0.0878	30.7511
• High RH	-0.4852	-0.3511	55.1593	-0.5958	-0.4233	66.0338
Speaking Three						
• Low RH	-0.3990	-0.0589	27.9199	-0.4899	-0.0683	33.1625
• Medium RH	-0.6921	-0.1629	51.4679	-0.9694	-0.2130	69.32ty34
• High RH	-0.7873	-0.4918	79.0972	-1.0096	-0.6153	98.4088

Predictions for coughing activity (Fig. 3) have comparable performance between the One and Three class approach for RH = 35 % in both summer and winter temperatures. Both approaches show similar values for the metrics considered, despite the tendency to underestimate the actual values as indicated by negative MBE (Table 5). In contrast, for RH = 55 %, the Three class approach substantially outperforms the One class, exhibiting improved estimates based on MBE with smaller MAE and larger R^2 values (Table 5). Given the Three Class approach better predictability, particularly at higher RH, the long-range airborne probability is predicted using it when determining the quanta emission rate (E_q).

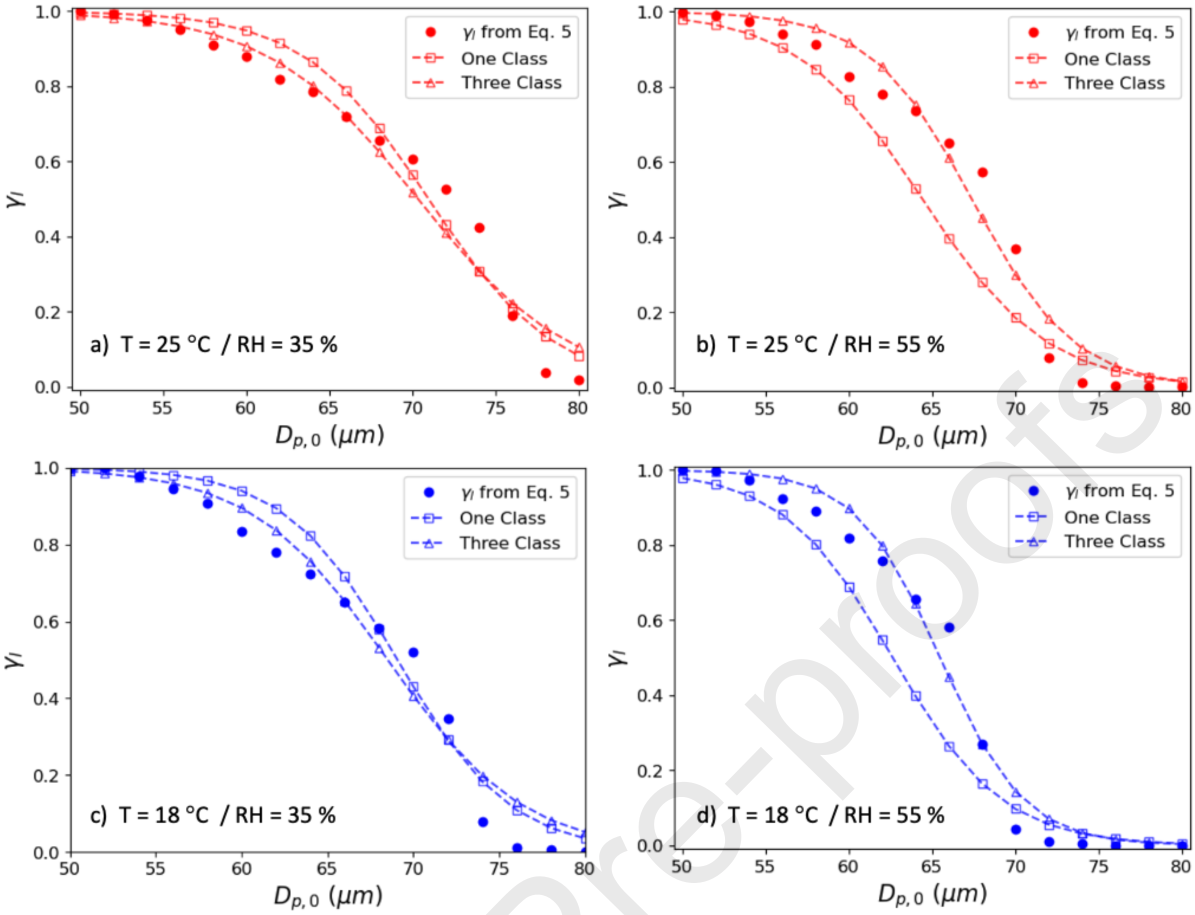

Figure 3. Long-range airborne probability when RH is (a, c) 35 % and (b, d) 55 % for (a, b) summer and (c, d) winter temperatures during coughing simulated using full model from Eq. 5 (circle), One (square) and Three Class (triangle) RH approaches fit to Eq. 6.

Table 5. Metrics (Section 2.2.1) used to evaluate cases when the RH is 35 and 55 %, with summer and winter temperatures, using One and Three RH class approaches.

Model		**RH = 35 %**			**RH = 55 %**		
		MAE	**MBE**	**R^2**	**MAE**	**MBE**	**R^2**
Summer	One	0.055	-0.023	0.959	0.092	0.070	0.894
	Three	0.046	0.000	0.963	0.049	-0.002	0.975
Winter	One	0.058	-0.039	0.963	0.087	0.067	0.907
	Three	0.050	-0.020	0.970	0.038	-0.020	0.983

3.3 Quanta emission rate

Increasing temperature leads to an increase in E_q, while higher RH results in a decrease in E_q. Coughing indoors has a 10-fold larger E_q if the RH is 20 % rather than 90 % (Fig. 4a), whilst for speaking the difference is only 2-fold for the same temperature conditions (Fig. 4b). Given the long-range airborne probability (Fig. 2) indoor temperature also influences the quanta emission rate across all RH levels (Fig. 4), with a more pronounced effect in drier environment. At T = 25 °C, the quanta emission rate increases up to 19 % for coughing and 8 % for speaking (cf. T = 18 °C). By linearly extrapolating our data, environments with a lower temperature of T = 14 °C would experience a slight reduction in the quanta emission rate, with a 11 % decrease for coughing and 5 % decrease for speaking for drier environments, with smaller values observed at higher RH levels.

For speaking E_q is larger than for coughing (Fig. 4), due to its higher frequency of occurrence. However, E_q for coughing alone (assuming 9 coughs h^{-1}) constitute a substantial fraction of that for speaking, amounting to approximately 20 % in an environment with RH = 20 % and to 6 % in with RH = 90 %. Moreover, as a sick person may alternate between speaking and coughing, and also with higher frequency of coughing, this could potentially further increase E_q values.

It is noteworthy that much lower estimates of E_q are obtained using the original Buonanno et al. (2020) formulation with a D_{crit} of 10 µm assumed. This large discrepancy arises from our approach accounting for the influence of larger droplets, which are more susceptible to environmental conditions. Hence, including this effect points to a greater potential for disease transmission.

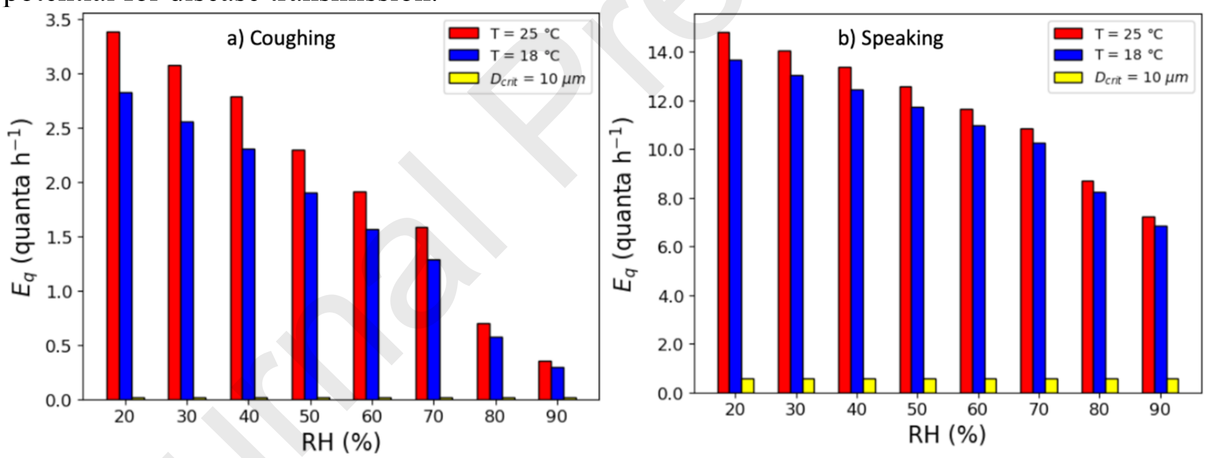

Figure 4. Quanta emission rate for different RH values for summer (red) and winter (blue) temperatures when (a) coughing and (b) speaking when D_{crit} = 100 µm, and if D_{crit} = 10 µm (yellow).

3.4 Case Study

In the following comparison, we explore the variability in calculated E_q using Monte Carlo simulation (1000 runs) for a retrospective method for two outbreak scenarios and our proposed method (Section 2.3). Due to the absence of specific temperature and relative humidity (RH) values during the outbreaks (Lu et al., 2020; Prentiss et al., 2020) we applied our proposed method to two extreme scenarios in terms of E_q estimates: dry and warm (RH = 20 % and T = 25 °C) and wet and cold (RH = 90 % and T = 18 °C). Additionally, we include the estimates using D_{crit} = 10 µm (Buonanno et al., 2020) and present the results in interquartile ranges (IQR) to illustrate the variability of the estimates while minimizing the influence of extreme values (Fig. 5).

From the retrospective analysis, for a 1-hour event in a restaurant in China the median value E_q of 32.76 quanta h^{-1} while it becomes 149.47 quanta h^{-1} in an 8-hour shift in a call centre in South Korea (green, Fig. 5). Although retrospective and prospective methods are not directly comparable, estimating E_q using our prospective model gives median E_q of 2.78 to 5.93 quanta h^{-1} for different environmental conditions, with lower values for when it is cold and wet (blue Fig. 5). Accounting for the environmental factors significantly influence quanta emission rates and provides a closer approximation to the retrospective data when compared to 0.21 quanta h^{-1} obtained using the upper limit D_{crit} = 10 µm as suggested by Buonanno et al. (2020) (yellow, Fig. 5).

By incorporating environmental variables, our model offers more accurate predictions of E_q. These results highlight the impact of seasonal and environmental factors. Recognizing these influences enables more robust risk assessments for airborne disease transmission and facilitates the development of targeted preventive measures, such as adjusting ventilation/heating strategies or implementing specific hygiene practices during high-risk periods.

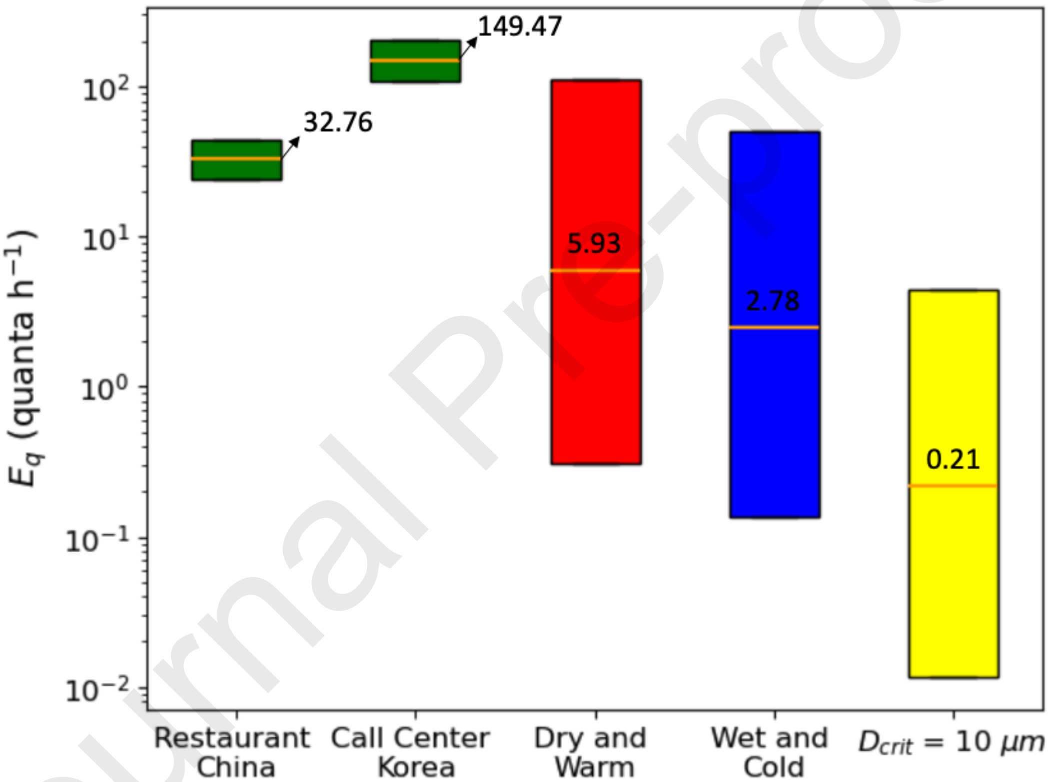

Figure 5. Quanta emission rate for two outbreak cases: a restaurant in China and a call centre in South Korea using the retrospective method(green). Dry and warm (T = 25°C, RH = 20 %, red) and wet and cold environment (T=18°C, RH = 90 %, blue) using our method alongside with the prospective method using D_{crit} = 10 µm. Note Y axis is nonlinear.

4. Limitations of this study

In our study, we calculate quanta emission rates without accounting for infectivity decays, ventilation or filtration after exhalation, rather we focus on particles remaining airborne without settling (deposition). However, once IRPs are expelled from the mouth, their infectivity and aerostability are affected by factors such as UV irradiation, ambient CO^2 concentration, temperature and relative humidity (Dabisch et al., 2021; Haddrell et al., 2024).

We consider a well-mixed stagnant indoor environment where ventilation does not directly affect the expired jet, yet ventilation designs could play an important role in mitigating airborne transmission risk (Bhagat et al., 2020). Targeted ventilation strategies, such as downward-directed airflows that enhance droplet settling could reduce airborne IRPs by increasing the surface deposition (Pandey et al., 2023). Similarly, prioritizing displacement ventilation over mixing ventilation, where feasible, may help limit fast dilution across the space and minimize the impact of ambient turbulence which could further increase the airborne residence time of droplets (Sodiq et al., 2021; Wei & Li, 2015). In both scenarios, decreasing ambient temperature could further minimise quanta concentrations.

In our study, we define the threshold distance between short and long-range transmission as 2 m for speaking and 4 m for coughing. While there are no absolute values distinguishing these transmission modes, our choice was based on common assumption that close-proximity for speaking falls within 1.5 – 2 m (Y. Li, 2021b), and that the cough jet can remain suspended in the air for longer compared to speaking breaths, reaching up to 4 m (Bourouiba, 2020). Beyond those distances, we assume droplet concentrations become well mixed in the environment, although in real-world conditions droplet distributions are often uneven and unsteady.

Although quanta emission rates are highly sensitive to viral load in droplets, we assume a constant viral load based on viral load of SARS-CoV-2 as in sputum, despite subject characteristics and contamination stage causing variation between 10^1 to 10^{11} RNA copies mL^{-1}, being an important source of uncertainty for quanta calculations (Pan et al., 2020). This assumption extends to all droplet sizes despite evidence suggesting that viral load of SARS-CoV-2 varies with droplet size and that finer droplets (< 5 μm) can carry up to 85 % of the total viral load in some cases across various SARS-CoV-2 variants (Coleman et al., 2022; Tan et al., 2023). These findings could significantly influence quanta emission rates calculations, with a comprehensive analysis across a wider range of droplet sizes and pathogens still being necessary. However, by not considering this variability, our findings are generalisable to other pathogens, which may not exhibit the same behaviour.

5. Conclusions

Quantifying the quanta emission rate is crucial for accurate assessment of infectious disease transmission risks. Here we propose a modified prospective method to estimate quanta emission rates that includes both environmental conditions and a larger threshold for inhalable droplet size. Our method employs the long-range airborne probability as a function of indoor relative humidity and temperature, and integrates it together with an exhalation droplet size distribution for coughing and speaking.

Our main findings are that both relative humidity and temperature are important factors in estimating quanta emission rates. Quanta emission rates can be up to 10 times larger in dry indoor environments (RH = 20 %) for coughing and 2 times larger for speaking modes compared to environments with RH = 90 %. Indoor air temperature has a large influence, particularly in dry conditions (RH = 20%) with winter scenario (T = 18 °C) having a 20 % higher quanta emission rate (cf. summer scenario). These effects are more pronounced for medium-sized droplets (40 – 70 μm), suggesting they could play a crucial role in the inhalation route of disease transmission.

6. Acknowledgements

VL acknowledges PhD studentship funding from NERC SCENARIO NE/S007261/1.

7. CRediT authorship contribution statement

Vitor Lavor: Writing - Original Draft, Methodology, Formal analysis, Visualization, Software. **Jianjian Wei**: Methodology, Investigation. **Omduth Coceal**: Supervision, Writing - Review & Editing. **Sue Grimmond**: Supervision, Writing - Review & Editing. **Zhiwen Luo**: Supervision, Conceptualization, Methodology, Writing - Review & Editing.

8. Declaration of competing interest

The authors declare that they have no known competing financial interests or personal relationships that could have appeared to influence the work reported in this paper.

References

Altshuler, E., Tannir, B., Jolicoeur, G., Rudd, M., Saleem, C., Cherabuddi, K., Doré, D. H., Nagarsheth, P., Brew, J., Small, P. M., Glenn Morris, J., & Grandjean Lapierre, S. (2023). Digital cough monitoring – A potential predictive acoustic biomarker of clinical outcomes in hospitalized COVID-19 patients. *Journal of Biomedical Informatics*, *138*, 104283. https://doi.org/10.1016/j.jbi.2023.104283

Bhagat, R. K., Wykes, M. S. D., Dalziel, S. B., & Linden, P. F. (2020). Effects of ventilation on the indoor spread of COVID-19. *Journal of Fluid Mechanics*, *903*, F1. https://doi.org/10.1017/jfm.2020.720

Bourouiba, L. (2020). Turbulent Gas Clouds and Respiratory Pathogen Emissions: Potential Implications for Reducing Transmission of COVID-19. *JAMA*, *323*(18), 1837–1838. https://doi.org/10.1001/jama.2020.4756

Buonanno, G., Robotto, A., Brizio, E., Morawska, L., Civra, A., Corino, F., Lembo, D., Ficco, G., & Stabile, L. (2022). Link between SARS-CoV-2 emissions and airborne concentrations: Closing the gap in understanding. *Journal of Hazardous Materials*, *428*, 128279. https://doi.org/10.1016/j.jhazmat.2022.128279

Buonanno, G., Stabile, L., & Morawska, L. (2020). Estimation of airborne viral emission: Quanta emission rate of SARS-CoV-2 for infection risk assessment. *Environment International*, *141*, 105794. https://doi.org/10.1016/j.envint.2020.105794

Cavazzuti, M., & Tartarini, P. (2023). Transport and evaporation of exhaled respiratory droplets: An analytical model. *Physics of Fluids*, *35*(10), 103327. https://doi.org/10.1063/5.0170545

Chaudhuri, S., Basu, S., Kabi, P., Unni, V. R., & Saha, A. (2020). Modeling the role of respiratory droplets in Covid-19 type pandemics. *Physics of Fluids*, *32*(6), 063309. https://doi.org/10.1063/5.0015984

Coleman, K. K., Tay, D. J. W., Tan, K. S., Ong, S. W. X., Than, T. S., Koh, M. H., Chin, Y. Q., Nasir, H., Mak, T. M., Chu, J. J. H., Milton, D. K., Chow, V. T. K., Tambyah, P. A., Chen, M., & Tham, K. W. (2022). Viral Load of Severe Acute Respiratory Syndrome Coronavirus 2 (SARS-CoV-2) in Respiratory Aerosols Emitted by Patients With Coronavirus Disease 2019 (COVID-19) While Breathing, Talking, and Singing. *Clinical Infectious Diseases: An Official Publication of the Infectious Diseases Society of America*, *74*(10), 1722–1728. https://doi.org/10.1093/cid/ciab691

Dabisch, P., Schuit, M., Herzog, A., Beck, K., Wood, S., Krause, M., Miller, D., Weaver, W., Freeburger, D., Hooper, I., Green, B., Williams, G., Holland, B., Bohannon, J., Wahl, V., Yolitz, J., Hevey, M., & Ratnesar-Shumate, S. (2021). The influence of temperature, humidity, and simulated sunlight on the infectivity of SARS-CoV-2 in aerosols. *Aerosol Science and Technology*, *55*(2), 142–153. https://doi.org/10.1080/02786826.2020.1829536

Duval, D., Palmer, J. C., Tudge, I., Pearce-Smith, N., O'connell, E., Bennett, A., & Clark, R. (2022). Long distance airborne transmission of SARS-CoV-2: Rapid systematic review. *Bmj*, *377*. https://www.bmj.com/content/377/bmj-2021-068743.long

Grandoni, L., Pini, A., Pelliccioni, A., Salizzoni, P., Méès, L., Leuzzi, G., & Monti, P. (2024). Numerical dispersion modeling of droplets expired by humans while speaking. *Air Quality, Atmosphere & Health*. https://doi.org/10.1007/s11869-024-01501-w

Gupta, J. K., Lin, C.-H., & Chen, Q. (2009). Flow dynamics and characterization of a cough. *Indoor Air*, *19*(6), 517–525. https://doi.org/10.1111/j.1600-0668.2009.00619.x

Haddrell, A., Oswin, H., Otero-Fernandez, M., Robinson, J. F., Cogan, T., Alexander, R., Mann, J. F. S., Hill, D., Finn, A., Davidson, A. D., & Reid, J. P. (2024). Ambient carbon dioxide concentration correlates with SARS-CoV-2 aerostability and infection risk. *Nature Communications*, *15*(1), 3487. https://doi.org/10.1038/s41467-024-47777-5

Haddrell, A., Otero-Fernandez, M., Oswin, H., Cogan, T., Bazire, J., Tian, J., Alexander, R., Mann, J. F. S., Hill, D., Finn, A., Davidson, A. D., & Reid, J. P. (2023). Differences in airborne stability of SARS-CoV-2 variants of concern is impacted by alkalinity of surrogates of respiratory aerosol. *Journal of The Royal Society Interface*, *20*(203), 20230062. https://doi.org/10.1098/rsif.2023.0062

Jimenez, J. L., Marr, L. C., Randall, K., Ewing, E. T., Tufekci, Z., Greenhalgh, T., Tellier, R., Tang, J. W., Li, Y., Morawska, L., Mesiano-Crookston, J., Fisman, D., Hegarty, O., Dancer, S. J., Bluyssen, P. M., Buonanno, G., Loomans, M. G. L. C., Bahnfleth, W. P., Yao, M., … Prather, K. A. (2022). What were the historical reasons for the resistance to recognizing airborne transmission during the COVID-19 pandemic? *Indoor Air*, *32*(8), e13070. https://doi.org/10.1111/ina.13070

Johnson, G. R., Morawska, L., Ristovski, Z. D., Hargreaves, M., Mengersen, K., Chao, C. Y. H., Wan, M. P., Li, Y., Xie, X., Katoshevski, D., & Corbett, S. (2011). Modality of human expired aerosol size distributions. *Journal of Aerosol Science*, *42*(12), 839–851. https://doi.org/10.1016/j.jaerosci.2011.07.009

Jones, B., Iddon, C., & Sherman, M. (2024). Quantifying quanta: Determining emission rates from clinical data. *Indoor Environments*, *1*(3), 100025. https://doi.org/10.1016/j.indenv.2024.100025

Jones, B., Iddon, C., & Sherman, M. H. (2023). *Quantifying Quanta: Why We Can't Be Certain About the Risks of Long-Range Airborne Infection* (SSRN Scholarly Paper No. 4595141). https://doi.org/10.2139/ssrn.4595141

Kroese, D. P., Brereton, T., Taimre, T., & Botev, Z. I. (2014). Why the Monte Carlo method is so important today. *WIREs Computational Statistics*, *6*(6), 386–392. https://doi.org/10.1002/wics.1314

Kurnitski, J., Kiil, M., Wargocki, P., Boerstra, A., Seppänen, O., Olesen, B., & Morawska, L. (2021). Respiratory infection risk-based ventilation design method. *Building and Environment*, *206*, 108387. https://doi.org/10.1016/j.buildenv.2021.108387

Leung, N. H. L., & Milton, D. K. (2024). New WHO proposed terminology for respiratory pathogen transmission. *Nature Reviews Microbiology*, *22*(8), 453–454. https://doi.org/10.1038/s41579-024-01067-5

Li, J., Cheng, Z., Zhang, Y., Mao, N., Guo, S., Wang, Q., Zhao, L., & Long, E. (2021). Evaluation of infection risk for SARS-CoV-2 transmission on university campuses. *Science and Technology for the Built Environment*, *27*(9), 1165–1180. https://doi.org/10.1080/23744731.2021.1948762

Li, Y. (2021a). Basic routes of transmission of respiratory pathogens—A new proposal for transmission categorization based on respiratory spray, inhalation, and touch. *Indoor Air*, *31*(1), 3–6. https://doi.org/10.1111/ina.12786

Li, Y. (2021b). Hypothesis: SARS-CoV-2 transmission is predominated by the short-range airborne route and exacerbated by poor ventilation. *Indoor Air*, *31*(4), 921.

Li, Y., Cheng, P., & Jia, W. (2022). Poor ventilation worsens short-range airborne transmission of respiratory infection. *Indoor Air*, *32*(1). https://doi.org/10.1111/ina.12946

Liu, L., Wei, J., Li, Y., & Ooi, A. (2017). Evaporation and dispersion of respiratory droplets from coughing. *Indoor Air*, *27*(1), 179–190. https://doi.org/10.1111/ina.12297

Lu, J., Gu, J., Li, K., Xu, C., Su, W., Lai, Z., Zhou, D., Yu, C., Xu, B., & Yang, Z. (2020). *COVID-19 Outbreak Associated with Air Conditioning in Restaurant, Guangzhou, China, 2020—Volume 26, Number 7—July 2020—Emerging Infectious Diseases journal—CDC*. *26*(7). https://doi.org/10.3201/eid2607.200764

Marr, L. C., & Tang, J. W. (2021). A Paradigm Shift to Align Transmission Routes With Mechanisms. *Clinical Infectious Diseases*, *73*(10), 1747–1749. https://doi.org/10.1093/cid/ciab722

Mikszewski, A., Stabile, L., Buonanno, G., & Morawska, L. (2022). The airborne contagiousness of respiratory viruses: A comparative analysis and implications for mitigation. *Geoscience Frontiers*, *13*(6), 101285. https://doi.org/10.1016/j.gsf.2021.101285

Miller, S. L., Nazaroff, W. W., Jimenez, J. L., Boerstra, A., Buonanno, G., Dancer, S. J., Kurnitski, J., Marr, L. C., Morawska, L., & Noakes, C. (2021). Transmission of SARS-CoV-2 by inhalation of respiratory aerosol in the Skagit Valley Chorale superspreading event. *Indoor Air*, *31*(2), 314–323. https://doi.org/10.1111/ina.12751

Milton, D. K. (2020). A Rosetta Stone for Understanding Infectious Drops and Aerosols. *Journal of the Pediatric Infectious Diseases Society*, *9*(4), 413–415. https://doi.org/10.1093/jpids/piaa079

Pan, Y., Zhang, D., Yang, P., Poon, L. L. M., & Wang, Q. (2020). Viral load of SARS-CoV-2 in clinical samples. *The Lancet Infectious Diseases*, *20*(4), 411–412. https://doi.org/10.1016/S1473-3099(20)30113-4

Pandey, B., Saha, S. K., & Banerjee, R. (2023). Effect of ceiling fan in mitigating exposure to airborne pathogens and COVID-19. *Indoor and Built Environment*, *32*(10), 1973–1999. https://doi.org/10.1177/1420326X231154011

Prentiss, M., Chu, A., & Berggren, K. K. (2020). *Superspreading Events Without Superspreaders: Using High Attack Rate Events to Estimate* N^{o} *for Airborne Transmission of COVID-19* (p. 2020.10.21.20216895). medRxiv. https://doi.org/10.1101/2020.10.21.20216895

Salthammer, T., & Morrison, G. C. (2022). Temperature and indoor environments. *Indoor Air*, *32*(5), e13022. https://doi.org/10.1111/ina.13022

Sodiq, A., Khan, M. A., Naas, M., & Amhamed, A. (2021). Addressing COVID-19 contagion through the HVAC systems by reviewing indoor airborne nature of infectious microbes: Will an innovative air recirculation concept provide a practical solution? *Environmental Research*, *199*, 111329. https://doi.org/10.1016/j.envres.2021.111329

Stadnytskyi, V., Bax, C. E., Bax, A., & Anfinrud, P. (2020). The airborne lifetime of small speech droplets and their potential importance in SARS-CoV-2 transmission. *Proceedings of the National Academy of Sciences*, *117*(22), 11875–11877. https://doi.org/10.1073/pnas.2006874117

Tan, K. S., Ong, S. W. X., Koh, M. H., Tay, D. J. W., Aw, D. Z. H., Nah, Y. W., Abdullah, M. R. B., Coleman, K. K., Milton, D. K., Chu, J. J. H., Chow, V. T. K., Tambyah, P.

A., & Tham, K. W. (2023). SARS-CoV-2 Omicron variant shedding during respiratory activities. *International Journal of Infectious Diseases*, *131*, 19–25. https://doi.org/10.1016/j.ijid.2023.03.029

Wei, J., & Li, Y. (2015). Enhanced spread of expiratory droplets by turbulence in a cough jet. *Building and Environment*, *93*, 86–96. https://doi.org/10.1016/j.buildenv.2015.06.018

Xie, X., Li, Y., Chwang, A. T. Y., Ho, P. L., & Seto, W. H. (2007). How far droplets can move in indoor environments ? Revisiting the Wells evaporation?falling curve. *Indoor Air*, *17*(3), 211–225. https://doi.org/10.1111/j.1600-0668.2007.00469.x

Highlights

- RH and temperature are important factors to estimate quanta emission rate (E_q)
- In dry environments, E_q for coughing increases ~10-fold and speaking 2-fold
- In dry summer conditions, higher temperature can increase E_q up to 22 %
- Medium-sized droplets may play a key role in infection transmission via inhalation

Vitor Lavor: Conceptualization, Methodology, Software, Formal analysis, Writing - Original Draft, Visualization; **Jianjian Wei**: Methodology, Writing - Review & Editing; Sue Grimmond: Methodology, Supervision, Funding acquisition, Writing - Review & Editing; **Omduth Coceal**: Methodology, Supervision, Funding acquisition, Writing - Review & Editing; **Zhiwen Luo**: Conceptualization, Methodology, Supervision, Funding acquisition, Writing - Review & Editing

Declaration of competing interests

The authors declare that they have no known competing financial interests or personal relationships that could have appeared to influence the work reported in this paper.